Supporting Information :

Fractional and Integer Charge Transfer at Semiconductor/Organic Interfaces: The Role of Hybridization and Metallicity

Simon Erker and Oliver T. Hofmann*

Institute of Solid State Physics, Graz University of Technology, NAWI Graz, Austria

E-mail: o.hofmann@tugraz.at

Further Details on the Applied Computational Methods

In this section we give additional computational details that were not mentioned in the main part of this publication. In particular, we want to explain how doping and the corresponding band-bending are considered in our DFT calculations and how we choose the initial charge density at the beginning of the self-consistent field cycle.

In principle, with choosing a hybrid functional containing a certain amount exact exchange in a DFT calculation, the solution for the transferred charge being localized on individual molecule (integer charge transfer, ICT) *and* the solution for charge being homogeneously distributed on all molecules (fractional charge transfer, FCT) can be obtained[1] (See section below, where we discuss the influence of the exchange-correlation functional). Both charge transfer solution are fundamentally different: For ICT electrons are transferred

*To whom correspondence should be addressed

in integer numbers, resulting in a splitting of the spin-channels. The LUMO gets spit up in a singly occupied molecular orbital (SOMO) and a singly unoccupied molecular orbital (SUMO). This leads to a semiconducting band structure (no density at the Fermi energy). In contrast, for FCT the spin channels stay degenerate as all molecules get fractionally charged. This leads to a quasi-metallic density of states. Therefore, a prerequisite to obtain the ICT solutions is to perform spin-polarized calculations (unrestricted, which increases the computational cost). As both charge transfer mechanisms are stable solutions in our DFT calculation, we enforced either solution be choosing the "right" initial charge density. FCT solutions were initialized with a fully spin-symmetric charge density. For the ICT solution the symmetry breaking of the spin channels can be enforced by an unsymmetric initial spin density. For that, we define individual molecules within our unit cell to have a non-vanishing initial moment (0.1 per atom). This allows us to select which molecules preferably end up with an extra electron. The breaking of the spin-density in the molecular layer and the coexistence of molecules with filled and empy LUMOs in the supercell is accompanied by a spontaneous breaking in translation symmetry. The geometry of a molecule with empty LUMO differs from the geometry of the molecule with a filled SOMO. Therefore, geometry relaxations on the same theoretical level (same density functional) for the whole molecular layer within the supercell are an essential part of correctly describing the charge transfer mechanism and the resulting effects.

Considering Doping of Semiconductors in our DFT Calculations

A special focus of this work is on how an organic/inorganic interface system behaves as the charge carrier concentration of the substrate is changed. Therefore, explicitly including doping in our DFT calculation of hybrid interfaces is of utmost importance for this work. We include bulk doping of the ZnO substrate in our calculations by using our recently developed CREST method[2,3]. CREST allows explicitly considering doping in DFT calculations by mimicking the long-ranged electrostatic effect of band-bending. In this approach doping

within the slab itself is introduced by means of the virtual crystal approximation (VCA).[4,5] In the VCA some of the bulk atoms are replaced by pseudo-atoms whose nuclear charge Z' (and the corresponding electron number) is fractionally altered from the bulk atom integer number Z. The added or subtracted fraction of charge, ΔZ, is set such that it corresponds to the desired bulk charge carrier concentration of the substrate. In our case of n-doped ZnO only the oxygen atoms in the slab are replaced by the pseudo-atoms with a fractional atomic number $Z' = Z + \Delta Z$. The additionally introduced change ΔZ per oxygen atom gives rise to excess electrons, which fill the bottom of the conduction band, resulting in a corresponding amount of mobile electrons. The counter charge remains spatially fixed at the ionic cores. This mobile charge carriers are then available to be eventually transfered into a molecular layer. The spatially fixed ionized cores build up the electric field that leads to band-bending. However, at lower charge carrier concentrations the size of the space-charge region drastically exceeds the size of a computational feasible slab. Therefore a different approach is necessary to treat the region below the slab. In CREST a charge-sheet is introduced below the slab that mimics the electrostatic field associated with band-bending. In practice the sheet is build up by a grid of positive point charges. We use a total of 480 equally distributed point charges for the charge-sheet in the 2×2 supercell (i.e., a grid of 3×5 point charges for the primitive surface unit cell with the dimensions 3.26×5.26 Å. This corresponds to a density of 0.87 point charges per Å^2). Along with the charge-sheet, the corresponding amount of electrons are introduced such that the system remains overall neutral. The additional electrons represent the bulk charge carrier concentration that is transfered to the interface. The distance of this charge-sheet from the slab and the amount of charge within the sheet is determined self-consistently, requiring the bottom side work functions to coincide with the bottom side work function of the ZnO slab without a molecular layer (i.e. without charge transfer or band-bending). The work function of the unperturbed slabs were determined for each doping concentration separately and a work function accuracy of 100 meV was required in the self-consistent CREST scheme. With this procedure we assure to obtain the correct

amount of charge transfer into the molecular layer at a specific charge carrier concentration and reproduce the charge-transfer-limiting effect of the band-bending. As described in more detail in the original publication,[2] the only input we need for CREST is the desired bulk charge carrier concentration and the dielectric constant ϵ_r of the ZnO substrate. In this work we use $\epsilon_r = 4.0$, which is agreement with experimental values of the high frequency dielectric constant of ZnO.[6]

At this point it should be emphasized that with the CREST approach a homogeneous bulk charge carrier concentration is considered without the explicit introduction of defect sites in the ZnO substrate. Surface or sub-surface defects, which are not explicitly considered, might drastically reduce the band-bending. Such defects can additionally influence the local potential at the surface and therefore locally alter the charge transfer and the charge transfer mechanism.

Surface Geometry and Monolayer Structure

We constructed a reasonable molecular monolayer structure of F4TCNQ molecules adsorbed on the mixed terminated ZnO (10-10) surface without performing a full structure search. We like to mention that there are advanced methods to predict the morphology of monolayers available or currently under development,[7,8] but for our conceptional study such an intensive search is not required. We used a simpler, more straight-forward process to find the monolayer structure. Starting from the lowest energy local adsorption site of a single molecule on the surface (which was found by chemical intuition, see below), we build the densest possible monolayer that only contains this geometry. The calculations to find the monolayer structure were performed with the PBE functional, which is computationally more efficient than hybrid functions. For the local adsorption site we used specific starting geometries motivated by chemical intuition and performed a geometry relaxation for the molecule only, fixing the substrate atoms at their initial position. We found that the cyano groups of the

molecule prefer binding to surface Zn atoms, that act as docking sites for the molecule. We looked at upright-standing as well as flat-lying adsorption geometries. For a single molecule the flat-lying geometries are energetically favorable. The two lowest-energy local adsorption sites are plotted in Fig. S1.

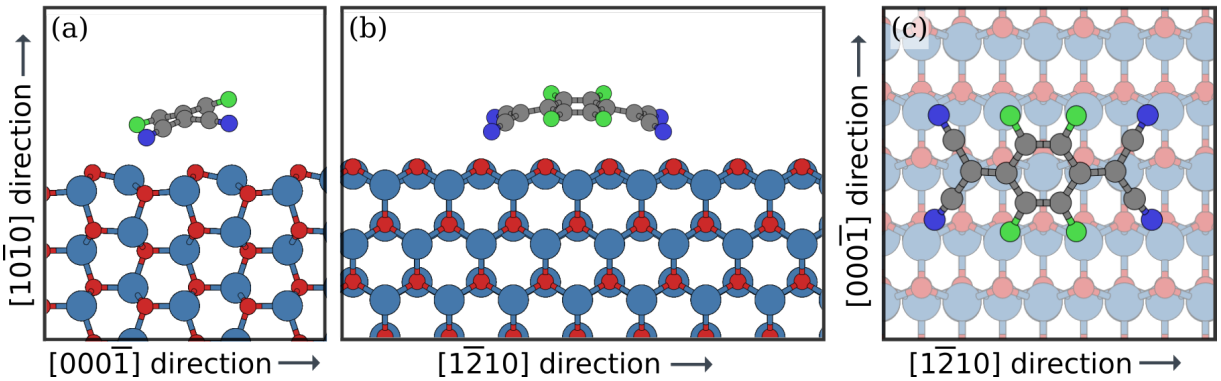

Figure S1: Adsorption geometry found for F4TCNQ on ZnO (10-10): (a-b/c) Side-view/topview of the lowest energy local adsorption site, that was further on used in this work to build the monolayer surface structure.

The energetically preferred adsorption site for the F4TCNQ molecule is parallel to the rills of the ZnO surface (parallel to the [11$\bar{2}$0] direction). In this configuration each of the four cyano groups can bind to surface Zn atoms and the molecule covers a surface of six Zn atoms in total. The smallest surface unit cell in this case is then a orthogonal unit cell comprised of six surface zinc and six surface oxygen atoms, with the dimensions of 13.05 Å $\times$ 10.41 Å in the [11$\bar{2}$0] and [0001] directions, respectively. From the smallest surface unit cell for a single molecule we build the monolayer structure by using this unit cell in a periodic slab approach. This means the applied coverage is defined by the structure of the ZnO surface, and we used the highest packing density allowing the commensurate adsorption of F4TCNQ in a flat-laying manner. For the bigger unit cell containing four molecules, a 2×2 supercell was used (See Fig. S2). We do not claim the monolayer morphology considered in this work to be the one that should be found in experiments.

We calculated the adsorption energy ΔE^{ads} of the F4TCNQ molecule on the undoped

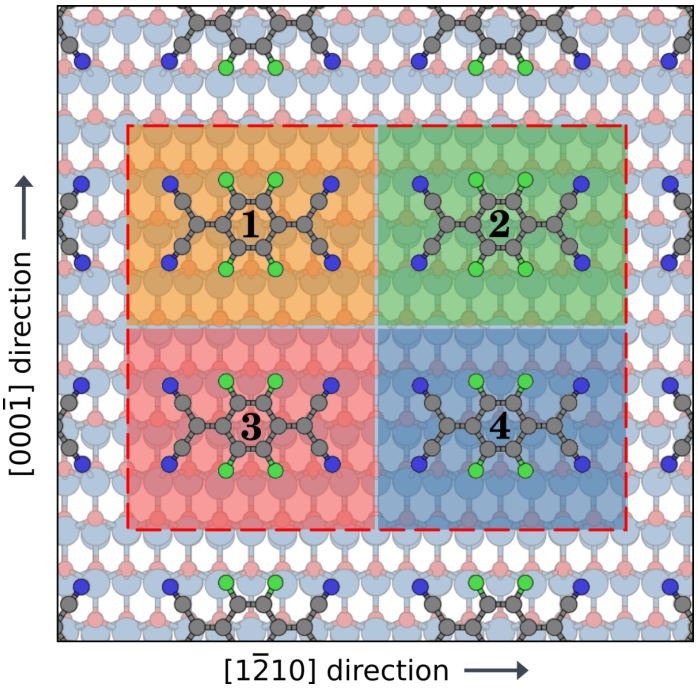

Figure S2: The red dashed line indicates the 2×2 supercell containing four molecules used in this work for the F4TCNQ monolayer on ZnO (10-10)

ZnO (10-10) surface using the following equation:

$$\Delta E^{\text{ads}} = E^{\text{sys}} - E^{\text{sub}} - E^{\text{mol}} \tag{1}$$

where E^{sys} and E^{sub} are the total energies of the combined system and the bare substrate, and E^{mol} is the total energy of the neutral molecule. The energy for the combined system was calculated from a PBEh ($\alpha = 0.63$) calculation with the small unit cell containing one molecule and the relaxation strategy described in the methods section of the main publication. The energy for the bare substrate was calculated in an equivalent manner without the adsorbate. The energy E^{mol} was obtained from a gas-phase calculation of the molecule. For the adsorption energy values neglecting van-der-Waals (vdW) interaction, we subtracted the vdW contribution to the total energies (the geometries were obtained including vdW interaction).

Molecular Orbital Density of States

In Fig. S3(a) we plot the molecular orbital density of states (MODOS) for the F4TCNQ molecule on undoped ZnO (10-10). Integration of each state up to the Fermi-energy then yields its formal occupation, as shown in Figure S3(b). The orbitals associated with the cyano groups (HOMO-10 to HOMO-13) show clearly a reduced occupation, because of the covalent bonding to surface Zn atoms. We find a notable occupation depletion of ca. 5%. This leads to a net positive charge transfer from this deeper laying states of 0.1 e- (value from Mulliken analysis of the cyano groups). For the other orbitals we find a rather weak hybridization with the substrate. The HOMO of the molecule is broadened to some extent. The LUMO basically does not hybridize at all with the bands of the semiconductor substrate, showing no broadening and remaining essentially empty (The nominal LUMO occupation of 2% and occupation numbers to be above 100%, that can be seen in Fig. S3(b), can be ascribed to artefacts of the Mulliken scheme).

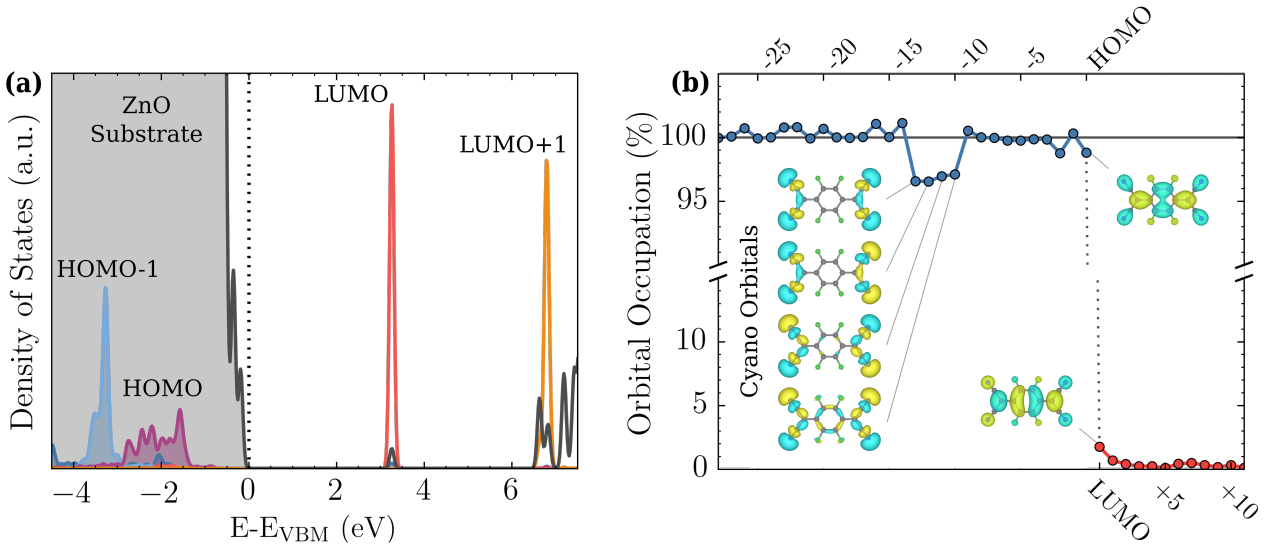

Figure S3: (a) Molecular orbital density of states (MODOS) projected on the free F4TCNQ orbitals and (b) molecular orbital population analysis of a single F4TCNQ molecule on undoped ZnO (10-10).

Discussion of the Applied Exchange-Correlation Functional: Determining the Hybrid Mixing Parameter

Describing the charge transfer, including the amount and particularly the localization of charge, is a non-trivial task using computational methods based on density functional theory (DFT). This is mainly attributed to the many-electron self-interaction error (MSIE) from which most approximate density functionals suffer.[9] This leads to a tendency of charge over-delocalization for common local and semilocal functionals. Therefore, these functionals favor FCT solutions for weakly hybridizing organic molecules adsorbed on inorganic substrates.[10] For describing the physics of such systems it is important to at least know whether the used functional does favor charge delocalization or localization.

In practice, the MSIE associated with approximate density functionals manifests itself as the convexity or concavity of the total energy as a function of fractional number of electrons N. In exact theory the ground-state energy with respect to N is known to be described by a series of straight-line segments.[11–13] The MSIE can, therefore, be defined indirectly using the straight-line energy condition.[11] A functional is defined as being free from many-electron SIE if the total energy $E(N)$ of an N electron system is a piecewise linear function between integer particle numbers. A deviation from this straight-line condition in form of a concave or convex E versus N curve is also referenced in the literature as localization error or delocalization error, respectively. Commonly used semilocal functionals underestimate the total energy of a system at factional occupation, leading to a convex energy curve and an over-delocalization of charge.[9,10,14] Hartree-Fock (HF), on the other hand, while being one-electron SI free by construction, still suffers from many-electron SI resulting in an overestimation of the total energy at factional occupation and charge over-localization.[9,10,14]

Because of this opposing trend for semilocal functionals and HF theory the deviation from the straight-line condition can be reduced and even lifted by employing a portion of the HF like exchange in a semilocal functional, resulting in so-called hybrid functionals.[15]

The disadvantage of such functionals is that they are computationally much more costly than their semilocal cousins. In this work, we apply the Perdew-Burke-Ernzerhof (PBEh) family of hybrid functionals:[16]

$$E_{xc}^{\mathrm{PBEh}} = \alpha E_x^{\mathrm{HF}} + (1-\alpha)E_x^{\mathrm{PBE}} + E_c^{\mathrm{PBE}} \tag{2}$$

for which the amount HF exchange can be tuned by the hybrid mixing parameter $\alpha \in [0,1]$ ($\alpha = 0$ corresponds to the common PBE functional,[17] the PBE0 functional is obtained by setting $\alpha = 0.25$[18,19]). The parameter α can be chosen to enforce the straight-line condition by requiring that the derivative of the total energy with respect to the number of electrons in the system, i.e. the orbital energy, does not change between integer electron numbers. This criterion can be enforced, for example, between the neutral and the singly-ionized system. It has recently been shown that when using hybrid functional DFT with an optimized mixing parameter α^* (i.e., the value at which the functional becomes MSIE-free), both solutions, the ICT and the FCT case, are stable and energetically degenerate if the straight line condition is fulfilled.[1] This limits our possibility to use DFT to predict the correct charge transfer mechanism, but gives us the opportunity to gain a deeper insight into charge transfer systems by studying both possible solutions. Therefore, our study should be seen as a proof of concept that both charge transfer mechanisms can in principle occur simultaneously.

In the following we show how we determined the mixing parameter α used in this work. We used the fact that the hybrid mixing parameter can be chosen to enforce the straight-line condition by requiring that the derivative of the total-energy with respect to the number of electrons in the system (in Kohn-Sham DFT this equals the energy of the orbital $\epsilon(N)$ that is filled) does not change between integer electron numbers N. We enforced this criterion for the free F4TCNQ molecule between the neutral and the singly-charged system and obtained the optimal mixing parameter $\alpha^* = 0.63$ (For a specific system we denote the optimal mixing parameter that fulfills the straight-line condition as α^*). This is the mixing parameter that

is used throughout this work, although the surface system should require less HF exchange than the molecule in the gas phase due to screening effects of the substrate.[1] We note that at α values below 0.2 the energy level alignment of the system is qualitatively no longer reproduced correctly. There, the LUMO of the F4TCNQ molecule is shifted below the valence band of the ZnO substrate, leading to a spurious charge transfer to the molecule already without doping. Therefore, possibly not all aspects of the F4TCNQ/ZnO interface can simultaneously be described correctly using hybrid functional DFT. To reproduce the correct energy level alignment, we need to accept that the charge localization for the chosen α parameter is driven towards over-localization and the integer charge transfer solutions are energetically favored by the applied functional. In other words, we apply the gas phase parameter because if using the α^* for the interface system (which would be less than 0.2) we obtain a spurious energy level alignment between the molecule and the substrate. We want to stress here that the qualitative results in this contribution are not influenced by the used functional as long we use a mixing parameter $\alpha > 0.2$ and a correct energy level ordering is assured. We tested that qualitatively equivalent results are obtained when using $\alpha = 0.25$, which is the default value for the PBE0 functional.[18,19]

Straight-Line Condition for F4-TCNQ in the Gas Phase

Determining the straight-line mixing parameter α^* for gas phase molecules using a DFT code capable of applying open boundary conditions is a straight forward procedure. We calculated the molecular orbital energies for the neutral molecule and the anion (i.e. singly charged molecule) using the optimized geometries of for various mixing parameters α. As FHI-aims allows to calculate fractional occupations of the orbital energies as well we can directly observe the concavity or convexity for the total energy curve (see Fig. S4). For PBE ($\alpha = 0.0$) the curve is clearly convex and for HF exchange ($\alpha = 1.0$) the curve is clearly concave. The total energies of the neutral molecule for every α are set to zero in this graph. We can also see that the electron affinity (EA) calculated from the total energy difference

between the anion and the neutral molecule obviously slightly depends on the amount of HF exchange, as the curves for the different αs do net meet again for the single negatively charged molecule.

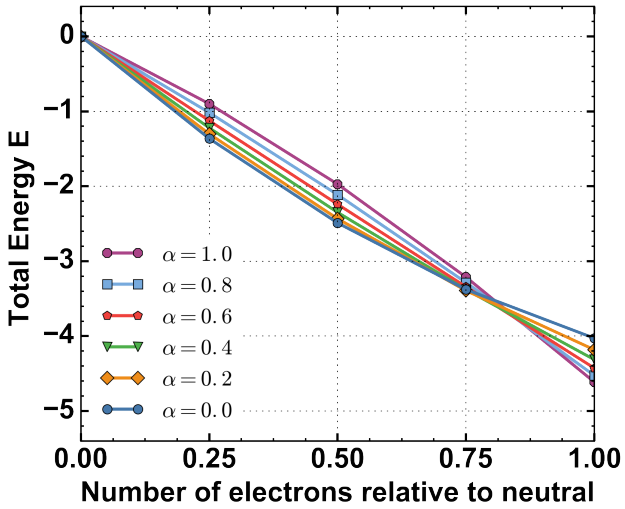

Figure S4: Total energy as a function of LUMO occupation between a neutral molecule and a anion for various hybrid mixing parameters α. Five charging levels have been considered ($N = 0$, $N = 0.25$, $N = 0.5$, $N = 0.75$ and $N = 1$). The energy curves are aligned to be zero for the neutral molecule.

To determine the optimal mixing parameter α^* we use the orbital energy of the LUMO (i.e. the derivative of the total energy curve). For a singly charged molecule, the LUMO of the neutral molecule now becomes the SOMO of the charged molecule. The energetic evolution of the LUMO as it becomes filled is plotted in Fig. S5(a) for various mixing parameters α. In agreement with the total energy curves we find a increase of the LUMO orbital energy as is become occupied for small mixing values $\alpha < 0.6$ and an decrease for higher mixing values $\alpha > 0.8$. The slope of the orbital energies are obtained from a linear fit and plotted in Fig. S5(b). A linear interpolation between the points results in a vanishing slope at the straight-line mixing parameter $\alpha^* = 0.63$. This is similar to the value of 0.7 obtained for the chemically similar TCNQ molecule.[15]

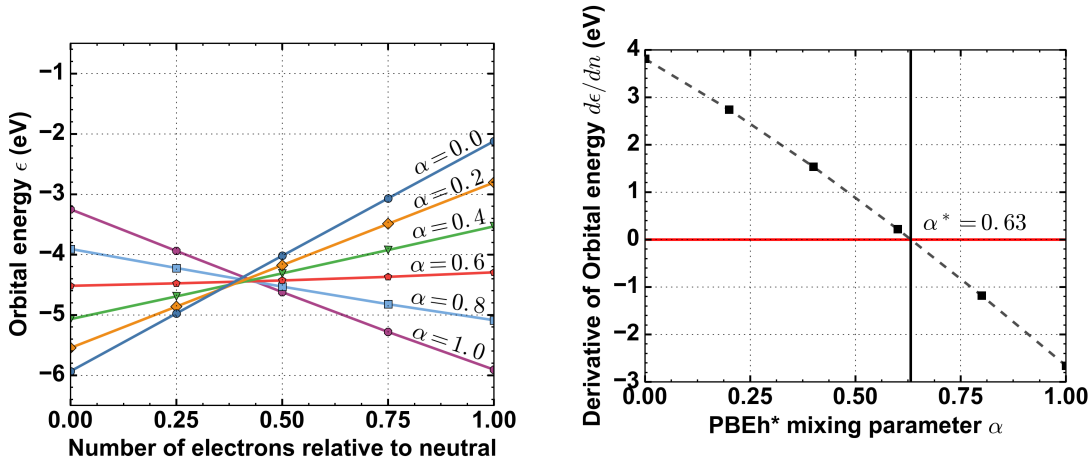

Figure S5: (left) Evolution of LUMO orbital energy of F4TCNQ in the gas phase as is gets (partially) occupied for different hybrid mixing parameters α. (right) Slope of the orbital energy plotted as a function of α. At $\alpha^* = 0.63$ the slope is zero and the straight line condition is fulfilled.

References

(1) Wruss, E.; Zojer, E.; Hofmann, O. T. Distinguishing between Charge-Transfer Mechanisms at Organic/Inorganic Interfaces Employing Hybrid Functionals. *The Journal of Physical Chemistry C* **2018**, *122*, 14640–14653.

(2) Erker, S.; Rinke, P.; Moll, N.; Hofmann, O. T. Doping Dependence of the Surface Phase Stability of Polar O-terminated $(000\bar{1})$ ZnO. *New Journal of Physics* **2017**, *19*, 083012.

(3) Sinai, O.; Hofmann, O. T.; Rinke, P.; Scheffler, M.; Heimel, G.; Kronik, L. Multiscale Approach to the Electronic Structure of Doped Semiconductor Surfaces. *Phys. Rev. B* **2015**, *91*, 075311.

(4) Nordheim, L. Zur Elektronentheorie der Metalle. I. *Annalen der Physik 401*, 607–640.

(5) Sinai, O.; Kronik, L. Simulated doping of Si from First Principles Using Pseudoatoms. *Phys. Rev. B* **2013**, *87*, 235305.

(6) Ashkenov, N.; Mbenkum, B. N.; Bundesmann, C.; Riede, V.; Lorenz, M.; Spemann, D.; Kaidashev, E. M.; Kasic, A.; Schubert, M.; Grundmann, M.; Wagner, G.; Neumann, H.;

Darakchieva, V.; Arwin, H.; Monemar, B. Infrared Dielectric Functions and Phonon Modes of High-Quality ZnO Films. *Journal of Applied Physics* **2003**, *93*, 126–133.

(7) Scherbela, M.; Hörmann, L.; Jeindl, A.; Obersteiner, V.; Hofmann, O. T. Charting the Energy Landscape of Metal/Organic Interfaces via Machine Learning. *Phys. Rev. Materials* **2018**, *2*, 043803.

(8) Packwood, D. M.; Han, P.; Hitosugi, T. Chemical and Entropic Control on the Molecular Self-Assembly Process. *Nature Communications* **2017**, *8*, 14463.

(9) Mori-Sánchez, P.; Cohen, A. J.; Yang, W. Many-Electron Self-Interaction Error in Approximate Density Functionals. *The Journal of Chemical Physics* **2006**, *125*, 201102.

(10) Mori-Sánchez, P.; Cohen, A. J.; Yang, W. Localization and Delocalization Errors in Density Functional Theory and Implications for Band-Gap Prediction. *Physical review letters* **2008**, *100*, 146401.

(11) Perdew, J. P.; Parr, R. G.; Levy, M.; Balduz, J. L. Density-Functional Theory for Fractional Particle Number: Derivative Discontinuities of the Energy. *Phys. Rev. Lett.* **1982**, *49*, 1691–1694.

(12) Perdew, J. P.; Ruzsinszky, A.; Csonka, G. I.; Vydrov, O. A.; Scuseria, G. E.; Staroverov, V. N.; Tao, J. Exchange and Correlation in Open Systems of Fluctuating Electron Number. *Phys. Rev. A* **2007**, *76*, 040501.

(13) Li, C.; Yang, W. On the Piecewise Convex or Concave Nature of Ground State Energy as a Function of Fractional Number of Electrons for Approximate Density Functionals. *The Journal of Chemical Physics* **2017**, *146*, 074107.

(14) Stein, T.; Autschbach, J.; Govind, N.; Kronik, L.; Baer, R. Curvature and Frontier Orbital Energies in Density Functional Theory. *The journal of physical chemistry letters* **2012**, *3*, 3740–3744.

(15) Atalla, V.; Zhang, I. Y.; Hofmann, O. T.; Ren, X.; Rinke, P.; Scheffler, M. Enforcing the Linear Behavior of the Total Energy with Hybrid Functionals: Implications for Charge Transfer, Interaction Energies, and the Random-Phase Approximation. *Phys. Rev. B* **2016**, *94*, 035140.

(16) Perdew, J. P.; Ernzerhof, M.; Burke, K. Rationale for Mixing Exact Exchange with Density Functional Approximations. *The Journal of chemical physics* **1996**, *105*, 9982–9985.

(17) Perdew, J. P.; Burke, K.; Ernzerhof, M. Generalized Gradient Approximation Made Simple [Phys. Rev. Lett. 77, 3865 (1996)]. *Phys. Rev. Lett.* **1997**, *78*, 1396–1396.

(18) Ernzerhof, M.; Scuseria, G. E. Assessment of the Perdew-Burke-Ernzerhof Exchange-Correlation Functional. *The Journal of Chemical Physics* **1999**, *110*, 5029–5036.

(19) Adamo, C.; Barone, V. Toward Reliable Density Functional Methods without Adjustable Parameters: The PBE0 Model. *The Journal of Chemical Physics* **1999**, *110*, 6158–6170.